

Ginsenoside Rg1 Ameliorates Pancreatic Injuries via the AMPK/mTOR Pathway in vivo and in vitro

Jin Chen^{1,*}, Guoping Zhu^{2,*}, Wenbo Xiao³, Xiaosong Huang⁴, Kewu Wang², Yi Zong² 

¹Department of Hematology, Yiwu Central Hospital, Yiwu, People's Republic of China; ²Department of Radiology, The Fourth Affiliated Hospital, Zhejiang University School of Medicine, Yiwu, People's Republic of China; ³Department of Radiology, The First Affiliated Hospital, Zhejiang University School of Medicine, Hangzhou, People's Republic of China; ⁴Department of Pharmacy, The Fourth Affiliated Hospital, Zhejiang University School of Medicine, Yiwu, People's Republic of China

*These authors contributed equally to this work

Correspondence: Kewu Wang; Yi Zong, Department of Radiology, The Fourth Affiliated Hospital, Zhejiang University School of Medicine, No. N1, Shangcheng Avenue, Yiwu, Zhejiang, People's Republic of China, Email 8016070@zju.edu.cn; zong@zju.edu.cn

Background: The main propanaxatriol-type saponin found in ginseng (*Panax ginseng* C. A. Mey), ginsenoside Rg1 (G-Rg1), has bioactivities that include anti-inflammatory, antioxidant, and anti-diabetic properties. This study aimed to investigate the effects of G-Rg1 on streptozotocin (STZ)-induced Type 1 Diabetes mellitus (T1DM) mice and the insulin-secreting cell line in RIN-m5F cells with high-glucose (HG) treatment.

Methods: The STZ-induced DM mice model was treated with G-Rg1 alone or combined with 3-Methyladenine (3-MA, an autophagy inhibitor)/rapamycin (RAPA, an autophagy activator) for 8 weeks, and levels of glucose and lipid metabolism, histopathological changes, as well as autophagy and apoptosis of relevant markers were estimated. In vitro, the HG-induced RIN-m5F cells were treated with G-Rg1, 3-MA, and Compound C (CC), an AMPK inhibitor, or their combinations to estimate the influences on cell apoptosis, autophagy, and AMPK/mTOR pathway-associated target gene levels.

Results: G-Rg1 treatment attenuated glucose and lipid metabolism disorder and pancreatic fibrosis in diabetic mice. In addition, subdued autophagy and p-AMPK protein expression, and enhanced p-mTOR protein expression and apoptosis levels in T1DM mice and HG-induced RIN-m5F cells were ameliorated by G-Rg1 treatment. Furthermore, these anti-apoptosis effects of G-Rg1 were partially abolished by 3-MA and CC.

Conclusion: Our findings revealed that G-Rg1 exhibits strong anti-apoptosis ability in pancreatic tissues of type 1 diabetic mice and HG-induced RIN-m5F cells, and the mechanisms involved in activating AMPK and inhibiting mTOR-mediated autophagy, indicating that G-Rg1 may have the therapeutic and preventive potential for treating pancreatic injury in diabetic patients.

Keywords: diabetes mellitus, ginsenoside Rg1, autophagy, apoptosis, AMPK

Introduction

Diabetes mellitus (DM) is a common disease worldwide, which is prone to long-term complications and endangers patients' health and its causes are mainly due to the damage of pancreatic islet cells that cannot secrete insulin properly or the development of insulin resistance in the body.¹ Type 1 diabetes mellitus (T1DM) is a chronic autoimmune disease mediated by T-lymphocytes in which the targeted destruction of pancreatic islet β -cells with increasing apoptosis levels, mostly in children and adolescents.^{1,2} According to the latest report published by the International Diabetes Federation (IDF), approximately 98,200 children and adolescents were diagnosed with T1DM each year.³ Also, the prevalence of T1DM in adults is increasing year by year in China.^{3,4} Moreover, there is no effective treatment for T1DM, and most T1DM patients are treated with continuous exogenous insulin supplementation as a lifelong treatment.⁵ Recently, there were many studies associated with islet transplantation, stem cell recovery, immune intervention, and insulin analogs, which provide new ideas in the treatment of T1DM.⁵⁻⁸ However, the compliance of purely Western medical treatment is poor and easily affects the quality of life of T1DM patients, which makes it difficult for many patients to achieve strict

control of blood glucose in daily life, resulting in significant blood glucose fluctuations and multiple complications.^{9,10} Furthermore, T1DM has been confirmed that it is related to various molecular mechanisms, including autophagy, oxidative stress, inflammation and apoptosis of pancreatic β -cells.^{11–13} Yet, though significant advances have been made since the past several decades, the potential therapeutic strategies and the exact molecular mechanisms of T1DM remain to be elucidated.

Autophagy is a form of autophagic cell death that recycles and recirculates nutrients by degrading damaged intracellular cytoplasm, organelles and protein aggregates and invading pathogens through the lysosomal pathway.^{11,14} Moderate autophagy can help maintain the number and the normal morphological structure of islet β -cells in the body with normal function.¹⁵ Autophagy can also delay apoptosis of pancreatic β -cells, while it can further protect pancreatic β -cells by adaptively reducing endoplasmic reticulum stress and then enhancing the survival of pancreatic β -cells.¹⁶ AMP-activated protein kinase (AMPK) is a key regulatory molecule of biological energy metabolism and a classical upstream regulator of autophagy, and activation of AMPK leads to the upregulation of autophagy.¹⁷ Studies have shown that AMPK is essential for islet β -cell survival and function in pancreatic tissue, and activation of AMPK mediates autophagy and improves islet β -cell function in diabetic mice.^{17–19} The mammalian target of rapamycin (mTOR), a downstream target of AMPK, can act as an intracellular nutrient sensor to regulate protein synthesis, cell growth, and metabolism.²⁰ With the progressive research on autophagy, the activation of pancreatic protective autophagy through the AMPK/mTOR pathway has attracted much attention from researchers as it weakens the apoptosis of islet β -cells.^{21,22}

Ginsenoside Rg1 (G-Rg1) is one of the main active components of *Ginseng*. And, studies have shown that G-Rg1 has a wide range of pharmacological effects such as anti-oxidative stress, anti-inflammatory, anti-aging, and neuroprotective.^{23,24} A study by Gao et al has shown that G-Rg1 improved streptozotocin (STZ)-mediated pyroptosis in the liver and pancreas of type 1 diabetic mice by regulating NLRP3 and Keap1/Nrf2/HO-1 signaling pathways.²⁵ In addition, G-Rg1 inhibited apoptosis by increasing autophagy through the AMPK/mTOR signaling pathway in serum deprivation of macrophages.²⁶ Therefore, we speculated that G-Rg1 has a protective and restorative effect on pancreatic β -cells in type 1 diabetic mice. Streptozotocin (STZ) was widely used to mediate DM that selectively damaged the insulin-producing islet β cells and, in turn, making a significant increase in free fatty acids (FFA) and hepatic triglycerides.²⁷ These findings might serve as a key mechanism for STZ-induced glucose and lipid metabolism dysregulation in T1DM. This study aimed to explore the preventive and curative effects of G-Rg1 on STZ-induced pancreatic lesions and the potential mechanisms of action in type 1 diabetic mice, especially on pancreatic autophagy activation, to provide a theoretical underpinning for the clinical treatment of G-Rg1 in T1DM.

Materials and Methods

Animals and Treatment

Six weeks old and weighing 22–25 g, fifty-five healthy SPF C57BL/6J mice were bought from the Beijing Vital River Laboratory Animal Technology Co., Ltd. (SCXK(Jing) 2021–0006, Beijing, China). The mice were given free access to food and water, kept at 23 °C to 25 °C with a relative humidity of 40% to 70%, and given a 12:12 h light: dark cycle. The administration of laboratory animals regulations were followed concerning the experimental animals and feeding procedures. After one week of adaptive feeding, mice were employed in later trials. For establishing diabetic models, forty-five mice were randomly selected and injected intraperitoneally with streptozotocin (STZ, Sigma, St Louis, USA) at a dose of 55 mg/kg once daily for 5 days as described in Lan et al.²⁸ The remaining 10 mice served as the control group and were injected intraperitoneally at the same time with equal amounts of biological physical saline. After 7 days of the injection, mice fasted for 10 h. Then, the fasting blood samples were collected from the tail vein to measure fasting glucose. Mice with glucose concentration > 16.7 mmol/L were considered type 1 diabetic mice. Subsequently, 40 selected mice were randomly divided into four groups, the model group (n=10), G-Rg1 group (n=10), G-Rg1 +3-Methyladenine (3-MA) group (n=10), and G-Rg1+Rapamycin (Rapa) group (n=10). In this study, mice in the G-Rg1, G-Rg1+3-MA, and G-Rg1+Rapa groups were gavaged daily with G-Rg1 (20 mg/kg/d, Shanghai Macklin Biochemical Co., Ltd, Shanghai, China). Based on prior researches, we administer STZ-induced T1DM mice with G-Rg1 (20 mg/kg/d) for 8 weeks as a pharmacological method.^{25,29} Also, mice in the G-Rg1+3-MA and G-Rg1+Rapa

groups underwent peritoneal injection of 3-MA (100 mg/kg/d) and Rapa (1.0 mg/kg/d, Shanghai yuanye Bio-Technology Co., Ltd, Shanghai, China), respectively.^{30,31} The control and model groups were orally administered the same volume of normal saline for 8 weeks. During the study, weekly measurements of the animal's body weight were measured until the experiment's conclusion. And, on the last day of G-Rg1, food intake and water intake were made recorded using metabolic chambers. At the end of week eight, the mice were fasted overnight and anesthetized by 45 mg/kg pentobarbitone sodium (Sigma-Aldrich, MO, USA), and the blood samples were collected from the orbital venous plexus using capillaries in plain tubes and centrifuged at 3000 rpm for 15 min at 4°C to obtain the serum for biochemical assays. Then, all mice were euthanized using the cervical dislocation protocol. After that, the pancreas tissues were quickly extracted and weighed for further experiments.

Determination of the HOMA-IR Index

During the test period, fasting blood glucose (FBG) levels were monitored weekly using a glucometer (Roche, Basel, Switzerland). In addition, the Ultra Sensitive Mouse Insulin ELISA kit (Meimian Industry, Yancheng, China) was used to assess the serum insulin level. Then, the homeostasis model of assessment for insulin resistance (HOMA-IR) index was calculated as $\text{FBG (mmol/L)} \times \text{Fasting insulin (FINS, mIU/L)} / 22.5$.³²

Oral Glucose Tolerance Test (OGTT)

After a 6-hour fast, a baseline blood draw from the tail vein was collected for plasma fasting glucose. Next, mice were gavaged with a glucose solution of 2 g/kg body weight, and blood samples from the tail vein were taken at 30, 60, 90, and 120 minutes to measure the blood sugar levels using an Accu-Chek glucometer. Using the OGTT results, the area under the curve (AUC) was obtained.

Biochemical Assays

The commercial kit for Hemoglobin A1c (HbA1c) was purchased from Beijing Leadman Biochemistry Co., Ltd (Beijing, China. Cat no. HA7430). Total cholesterol (TC), total triglycerides (TG), low-density lipoprotein cholesterol (LDL-C), and high-density lipoprotein cholesterol (HDL-C) kits were purchased from Nanjing Jian Cheng Corp., (NanJing, China. Cat no. A111-1, A110-1, A113-1, A112-1). Serum concentrations of HbA1c, TC, TG, LDL-C, FFA, and HDL-C levels were measured by use of an automatic biochemical analyzer (Hitachi 7080, Japan) according to the manufacturer's protocols. Free fatty acid (FFA) levels were measured with a non-esterified Free fatty acids assay kit (Nanjing Jiancheng, Nanjing, China. Cat no. A042-1).

Histopathology, TUNEL, Immunohistochemical (IHC) Analysis

At the end of the experiment, the pancreas of each mouse was quickly isolated after blood collection. The pancreas from mice in each group was obtained and fixed in 4% paraformaldehyde for 24 h at room temperature, embedded in paraffin, and sliced into 4 μm sections. The sections were prepared and used to perform hematoxylin-eosin (H&E), Masson, and Terminal Deoxynucleotidyl Transferase-Mediated dUTP Nick End-Labeling (TUNEL) staining according to the manufacturer's instructions. For immunohistochemical analysis, paraffin sections were routinely dewaxed and hydrated, antigen was repaired with citrate buffer, and endogenous peroxidase was closed with 3% H_2O_2 . Next, the sections were incubated with Rabbit anti-p-AMPK antibody (Affinity Biosciences, 1:200) or anti-p-mTOR antibody (Affinity Biosciences, 1:200). HRP-conjugated Goat Anti-Rabbit IgG (Abcam, ab97080, 1:5000) was used as secondary antibody for 30 min and visualized by the 3,3'-diaminobenzidine (Servicebio, G1212-200T). It was observed using an optical microscope (Nikon, Japan). Positive staining of TUNEL and IHC was quantified by Image Pro Plus software.

Transmission Electron Microscopy (TEM) Analysis

The tail of the pancreas was used, cut into small pieces of 1 mm \times 1 mm \times 1 mm in size, and fixed with a mixture of 2.5% glutaraldehyde and 2% osmium tetroxide. The tissue was gradient dehydrated and then fixed in epoxy resin. Ultrathin sections were sieved through a 200-mesh sieve. Sieved sections were stained with uranyl acetate and lead

acetate, and the morphology of autophagic structures was photographed under a Hitachi TEM system (Hitachi, Ltd., Tokyo, Japan) at 8.0 kV.

Cell Culture and Treatment

The rat pancreatic β cell line RIN-m5F was purchased from the Kunming Cell Bank of the Chinese Academy of Sciences and then grown in RPMI 1640 medium (Gibco, USA) containing 10% fetal bovine serum (FBS) (Gibco, USA) at 37 °C in a 5% CO₂ environment. Briefly, RIN-m5F cells were exposed to media containing a different or single concentration of G-Rg1 with 3-MA (2 mM) or Compound C (CC, 50 mM) or without 3-MA or CC as a control for 24h, followed by the treatment with 30 mM high glucose (HG) for 48 h. Then, the protein expression levels of autophagy, apoptosis, and AMPK/mTOR pathway-associated targets and cellular apoptosis were measured by Western blotting and flow cytometry analysis, respectively.

Cell Viability Assay

To expound the role of G-Rg1 on the cell viability of RIN-m5F cells, the Cell Counting Kit-8 (CCK-8) assay was performed according to the manufacturer's recommendations. Briefly, RIN-m5F cells were seeded in 96-well plates at a cell density of 5000 cells/well, and the cells were incubated at 37 °C for 24 h. Next, the cells were randomly divided into eight groups, and six replicate wells were set up in each group, and the cells were cultured with RPMI 1640 medium containing 0, 50, 100, 200, 300, 400, 500, and 600 μ M of G-Rg1 for 48h, in which 0 μ M of G-Rg1 group was used as blank control. Subsequently, 10 μ L of CCK-8 solution was added to each well of each group and then incubated at 37 °C for 2h. Finally, the relative survival rate of each group of cells was calculated by using a microplate reader to determine the optical density (OD) value of each well at a wavelength of 450 nm.

Immunofluorescence Assay

Fixed in 4% paraformaldehyde and mixed with 0.1% Triton X-100 for 15 min, the HG-induced RIN-m5F cells with G-Rg1 treatment were then blocked in 5% bovine serum albumin (BSA) for 1 h. Cells were exposed to the primary anti-LC3 antibodies listed below (ab192890, Abcam) at 4°C overnight, followed by secondary antibodies at 37°C for 1 h. After 4',6-diamidino-2-phenylindole (DAPI) staining, observations were made using an inverted fluorescent microscope.

Flow Cytometry Analysis

Using an Annexin V-FITC/PI apoptosis kit (BD Pharmingen, USA), the apoptosis of treated RIN-m5F cells was assessed following the manufacturer's instructions. The cells were gathered and twice washed in phosphate-buffered saline (PBS). After that, cells were incubated in 500 μ L of 1 \times binding buffer containing 5 μ L of Annexin V-fluorescein isothiocyanate (FITC) and 10 μ L of propidium iodide (PI) for 5 min in the dark. The next step was to identify apoptosis within 1 h using a flow cytometer (BD Biosciences, USA), and to generate the plot, the values for Annexin V and PI were placed as the horizontal and vertical axes, respectively.

Quantitative Real-Time PCR (qRT-PCR) Analysis

Total RNA of pancreatic tissues was isolated using Trizol reagent (Invitrogen, USA) and transformed into complementary DNA (cDNA) employing a cDNA synthesis kit (Beijing ComWin Biotech Co., Ltd., Beijing, China). QRT-PCR analysis was performed using SYBR Premix Ex Taq^{II} reagent on a CFX Connect system (BIO-RAD, USA), using the following reaction conditions: 1 cycle of 95°C for 5 min, 40 cycles at 95°C for 15s, and 60°C for 30s. Primers were synthesized by Sangon Biotech (Shanghai) Co., Ltd (Shanghai, China) and listed in Table 1. Finally, the 2^{- $\Delta\Delta$ Ct} method was used to analyze the expression level of the target genes relative to the β -actin.³³

Western Blot Analysis

Total protein of the pancreatic tissues and G-Rg1-treated RIN-m5F cells was extracted by RIPA buffer (Beijing ComWin Biotech Co., Ltd. China) at 4°C for 20 min and quantified by the bicinchoninic acid assay (Beyotime Biotechnology, China). Then, protein samples were separated by 8%–10% sodium dodecyl sulfate-polyacrylamide gel electrophoresis (SDS-PAGE) and transferred to a polyvinylidene difluoride (PVDF) membrane (GE Healthcare Life). Membranes were

Table 1 Primer Sequences for qRT-PCR Analysis

Name	Forward Sequence (5'-3')	Afterward Sequence (5'-3')
Beclin-1	ATGGAGGGGTCTAAGCGTC	TGGGCTGTGGTAAGTAATGGA
LC 3	TTATAGAGCGATACAAGGGGAG	CGCCGTCTGATTATCTTGATGAG
Bax	AGACAGGGCCTTTTTGCTAC	AATTCGCCGAGACTCG
Bcl-2	GAGCCTGTGAGAGACGTGG	CGAGTCTGTGTATAGCAATCCCA
Caspase-3	CTCGCTCTGGTACGGATGTG	TCCATAAATGACCCCTTCATCA
β -actin	ATGACCCAAGCCGAGAAGG	CGCCAAGTCTTAGAGTTGTTG

blocked by 5% skimmed milk powder for 2 h at room temperature. After that, the membranes were then incubated with primary antibodies of Beclin-1 (1:1000, Cell Signaling Technology), LC 3 (1:1000, Affinity Biosciences), p62 ((1:1000, Cell Signaling Technology), Bax (1:2000, Cell Signaling Technology), Bcl-2 (1:1000, Affinity Biosciences), Caspase-3 (1:500, Abcam), p-AMPK (1:1000, AF3423, Affinity Biosciences), AMPK (1:1000, AF6423, Affinity Biosciences), p-mTOR (1:1000, AF3308, Affinity Biosciences), mTOR (1:1000, AF6308, Affinity Biosciences), and β -actin (1:5000, AF7018, Affinity Biosciences) at 4°C overnight. Following three TBST washes, the PVDF membranes were incubated with horseradish peroxidase-conjugated secondary antibody at room temperature for 1.5 h. Finally, with the aid of a multifunctional imaging system, an enhanced chemiluminescent (ECL) kit was used to detect immunoreactive proteins. Image J software (National Institutes of Health) was used to quantify the signal from the protein bands, and the results were standardized to the β -actin.

Statistical Analysis

All data are presented as Means \pm SD. Statistical analysis was conducted using the SPSS statistical software. Two-tailed Student's *t*-tests were used to compare the differences between groups. The threshold for statistical significance was set at $P < 0.05$.

Results

G-Rg1 Ameliorated the General Symptom Through Autophagy in T1DM Mice

In this study, the autophagy inhibitor 3-MA and activator Rapa were used to investigate the effect of G-Rg1 in T1DM mice. We measured the glucose and lipid metabolism indicators to reveal the therapeutic role of G-Rg1 in vivo, it is evident that G-Rg1 has a tendency to increase weight (Figure 1A) and FINS levels (Figure 1E), while significantly decreasing food intake (Figure 1B), water intake (Figure 1C), FBG, and HOMA-IR levels (Figure 1D–E) when compared with the group model ($P < 0.01$). It is noteworthy that 3-MA greatly diminished the protective effect of G-Rg1, whilst its protective effect was significantly increased by Rapa (Figure 1A–E, $P < 0.01$). In terms of the OGTT test, the diabetic mice's blood glucose level dramatically rose within 30 min after oral glucose treatment, and the hyperglycemic state was prolonged in the mice of model and G-Rg1+ 3-MA groups. Furthermore, blood glucose levels in mice treated with G-Rg1 and G-Rg1+Rapa started to reduce after 60 min of the glucose challenge and significantly after 120 min. Also, the results of the AUC showed depraved glucose tolerance in the model and G-Rg1+3-MA groups, which was ameliorated by G-Rg1 combined with Rapa (Figure 1F, $P < 0.01$).

For additional evidence that G-Rg1 has a hypoglycemic effect, we also assessed the level of HbA1c in the serum of T1DM mice. After the intervention, the HbA1c level in the G-Rg1 and G-Rg1+Rapa groups were significantly lower than those in the model group, whereas the G-Rg1+3-MA group exhibited significantly higher HbA1c levels than the model group (Figure 2A, $P < 0.01$). To ascertain the impact of G-Rg1 on hyperlipidemia in T1DM mice, TC, TG, LDL-C, FFA, and HDL-C were examined at the end of the research process. Similar to the HbA1c results, the TC, TG, LDL-C, and FFA of G-Rg1 and G-Rg1 +Rapa groups significantly decreased compared to the model group. Meanwhile, the HDL-C level significantly increased in the G-Rg1 and G-Rg1+Rapa groups (Figure 2B–F, $P < 0.01$). These findings indicated that the effects of G-Rg1 on glucose and lipid metabolism were associated with autophagy in T1DM mice.

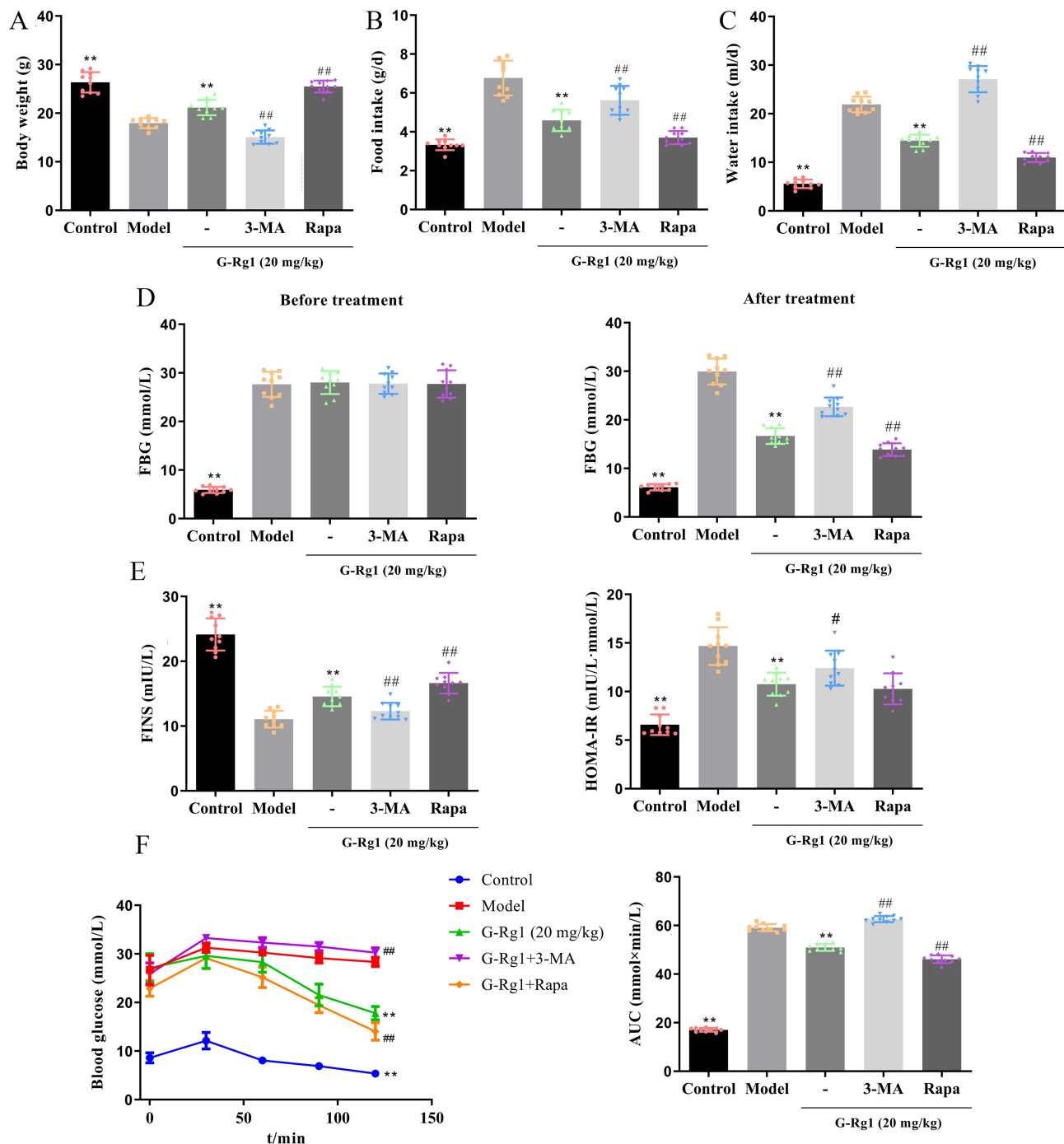


Figure 1 Effect of G-RgI on general conditions and glucose metabolism in STZ-induced diabetic mice. (A) Body weight, (B) food intake, and (C) water intake of STZ-induced diabetic mice were treated with G-RgI or combined with 3-MA or Rapa. (D) fasting blood glucose (FBG) of mice before and after G-RgI treatment. (E) Fasting insulin (FINS) levels in serum and Homeostasis model of assessment for insulin resistance (HOMA-IR) index. (F) Blood glucose levels and area under the curve (AUC) in the oral glucose tolerance test (OGTT). Data are shown as mean \pm SD. $n = 10$ per group. ** $P < 0.01$, compared with the model group; # $P < 0.05$, ## $P < 0.01$, compared with the G-RgI (20 mg/kg) group.

G-RgI Improved Pancreatic Injuries in T1DM Mice

As shown in Figure 3A–B, the pancreatic weight and the index of the G-RgI+Rapa groups were significantly lower than those of the model group. By contrast, the pancreatic weight and the index significantly decreased in the G-RgI+3-MA group. Pathohistological examination showed that the model and G-RgI+3-MA groups' pancreatic islets were disorganized, had fewer islet cells, and had smaller pancreatic islet diameters. Consistent with HE staining, we found that islet

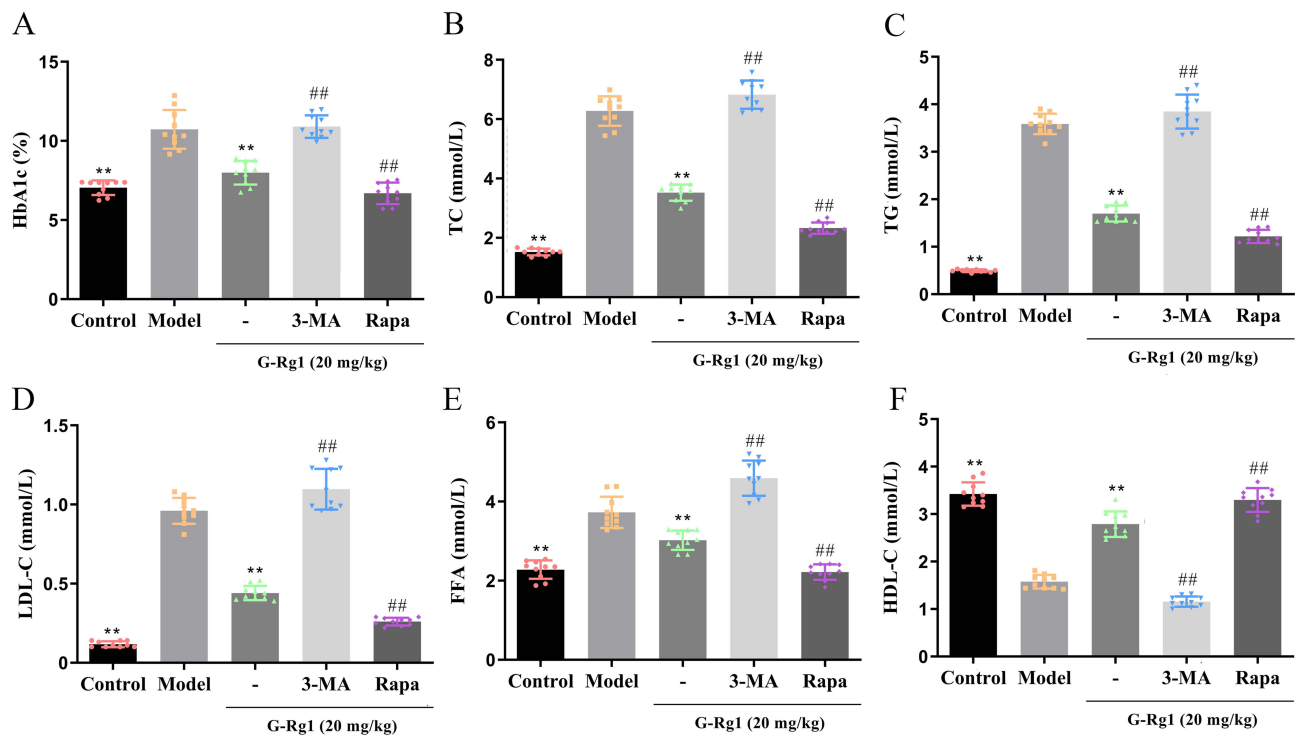


Figure 2 Effect of G-Rg1 on lipid metabolism in STZ-induced diabetic mice. (A) The serum levels of (A) HbA1c, (B) TC, (C) TG, (D) LDL-C, (E) FFA, and (F) HDL-C were estimated using an automatic biochemical analyzer. ** $P < 0.01$, compared with the model group; ### $P < 0.01$, compared with the G-Rg1 (20 mg/kg) group.

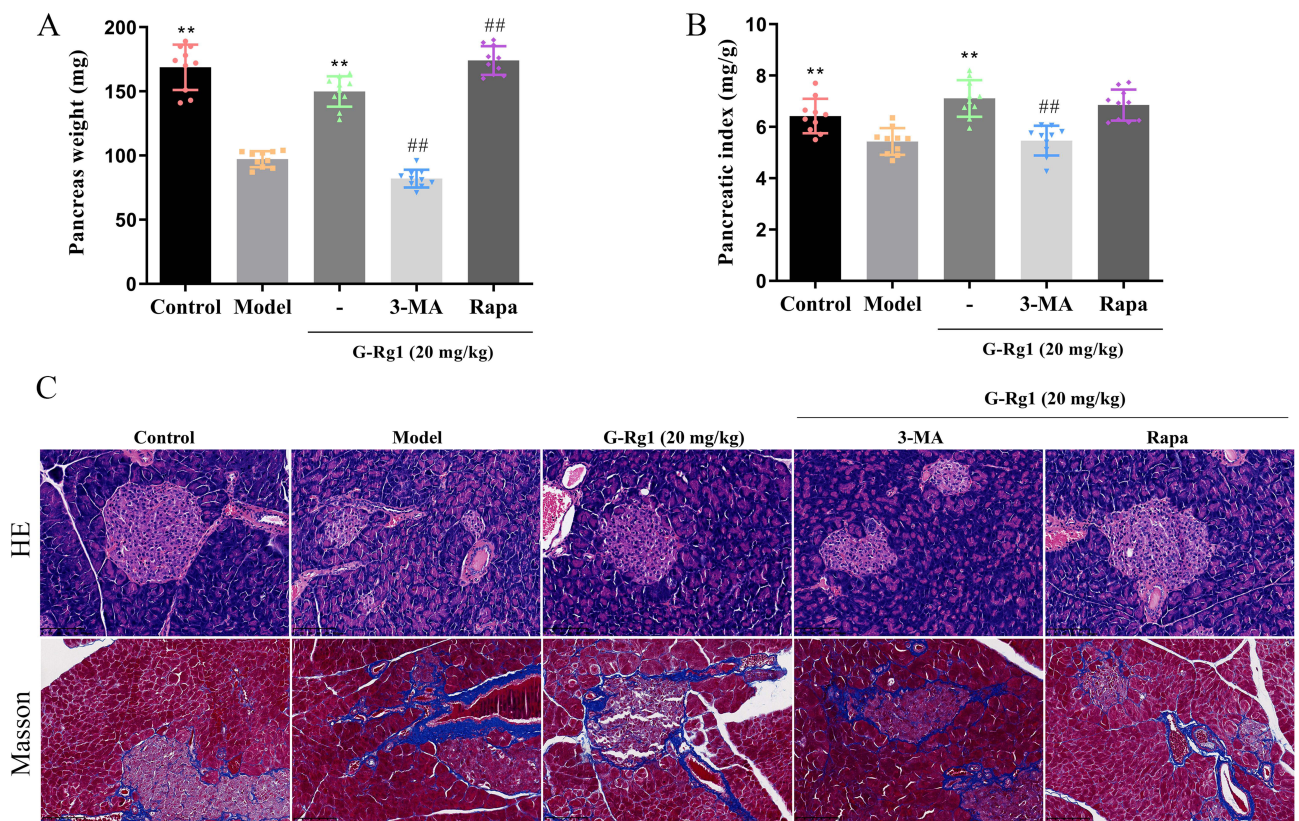


Figure 3 Effect of G-Rg1 on histopathology changes of pancreas in STZ-induced diabetic mice. (A) Pancreatic weight and (B) Pancreatic index. (C) The pathological changes of the pancreas were assessed by H&E and Masson staining (Magnification, $\times 200$). ** $P < 0.01$, compared with the model group; ### $P < 0.01$, compared with the G-Rg1 (20 mg/kg) group.

fibrosis within the islets was significantly increased in the model and G-Rg1+3-MA groups. In contrast, treatment with G-Rg1 and G-Rg1+Rapa in T1DM mice significantly reversed these effects (Figure 3C, $P<0.05$).

G-Rg1 Improved Defective Autophagy and Reduced Apoptosis of Pancreatic Tissue in T1DM Mice

To further confirm the role of G-Rg1 on autophagy and apoptosis in mice, we estimated the number of autophagosomes and the expression levels of autophagy and apoptosis-associated targets. The result of TEM illustrated that the number of autophagosomes in the G-Rg1 and G-Rg1+Rapa groups was markedly higher than that in the model group (Figure 4A and B, $P<0.05$). Compared with the model group, the higher expression levels of Beclin-1 and LC 3 were observed in the G-Rg1 and G-Rg1+Rapa groups, however, the number of autophagosomes, the expression levels of Beclin-1 and LC 3 were significantly inhibited in G-Rg1+3-MA group when compared with the G-Rg1 group (Figure 4C and D, $P<0.05$). We next used TUNEL labeling to detect islet apoptosis to ascertain if G-Rg1 helps maintain β -cell in STZ-induced T1DM mice. The number of TUNEL-positive β -cells was lower in mice of G-Rg1 and G-Rg1+Rapa groups than in model mice (Figure 4E and F, $P<0.01$). As shown in Figure 4G and H, the levels of Bax and Caspase-3 were reduced significantly in the pancreatic tissue of T1DM mice in G-Rg1 and G-Rg1+Rapa groups compared with that of the model group. Increased Bcl-2 level was observed in the G-Rg1 and G-Rg1+Rapa groups (Figure 4I, $P<0.01$). Representative protein bands of autophagy and apoptosis-associated targets are shown in Figure 4J, the results of Western blot were in agreement with the qRT-PCR assays. However, we also discovered that autophagy inhibitors were able to significantly lessen the protective effects of G-Rg1 on the death of pancreatic tissue in T1DM animals. All of these findings imply that the G-Rg1 prevented STZ-induced pancreatic-cell death in mice by promoting autophagy.

G-Rg1 Ameliorated the AMPK/mTOR Pathway Changes in the Pancreatic Tissue of T1DM Mice

Immunohistochemistry and Western blot analyses indicated that p-AMPK significantly reduced and p-mTOR over-expressed in the pancreatic tissue of T1DM mice ($P<0.01$). In our study, G-Rg1 and G-Rg1+Rapa administration significantly increased the expression of p-AMPK but decreased that of p-mTOR in the pancreatic tissue of T1DM mice (Figure 5A–C, $P<0.01$). Overall, these findings showed that the therapeutic impact of G-Rg1 treatment on suppressing pancreatic apoptosis is connected to the regulation of the AMPK/mTOR pathway.

G-Rg1 Decreased HG-Induced Apoptosis and Triggered Autophagy in RIN-m5F Cells

As illustrated in Figure 6A, cell viability of RIN-m5F cells was significantly decreased when challenged with G-Rg1 at a dose of 300, 400, 500, and 600 μ M after 24h ($P<0.01$), while there was no effect on the viability of RIN-m5F cells with 50, 100, 200 μ M of G-Rg1 treatment. To avoid cell death in vitro, the concentration of G-Rg1 in the following research was lower than 300 μ M. Surprisingly, the results of flow cytometry showed that the number of early and late apoptotic RIN-m5F cells was significantly higher in HG-induced apoptosis cells than in the control cells. Nevertheless, pretreatment with G-Rg1 significantly reduced the apoptosis rate of RIN-m5F cells as compared to HG-induced cells, as shown in the flow cytometry scatter plot (Figure 6B, $P<0.05$). We also checked the expression level of autophagy markers using immunofluorescence staining and Western blotting. Immunofluorescence staining results showed that the density of LC3 was dramatically increased in HG-induced RIN-m5F cells with G-Rg1 treatment (Figure 6C). Additionally, we also found that G-Rg1 increased the expression of Beclin-1 and the ratio of LC3 II/LC3 I, whereas decreased the expression of p62 in HG-induced RIN-m5F cells with dose dependence to a certain degree (Figure 6D, $P<0.05$). Taken together, these results suggested that G-Rg1 could activate autophagy in the HG-induced RIN-m5F cells.

G-Rg1-Mediated Autophagy Decreased Apoptosis in HG-Induced RIN-m5F Cells

Next, we further investigated whether G-Rg1-induced autophagy could attenuate RIN-m5F cell apoptosis. As shown in Figure 7A, G-Rg1 reduced HG-induced apoptosis of RIN-m5F cells was significantly promoted by the 3-MA, an early-stage autophagy inhibitor ($P<0.01$). Furthermore, 3-MA reduced the protein expression of Beclin-1, the ratio of LC3 II/

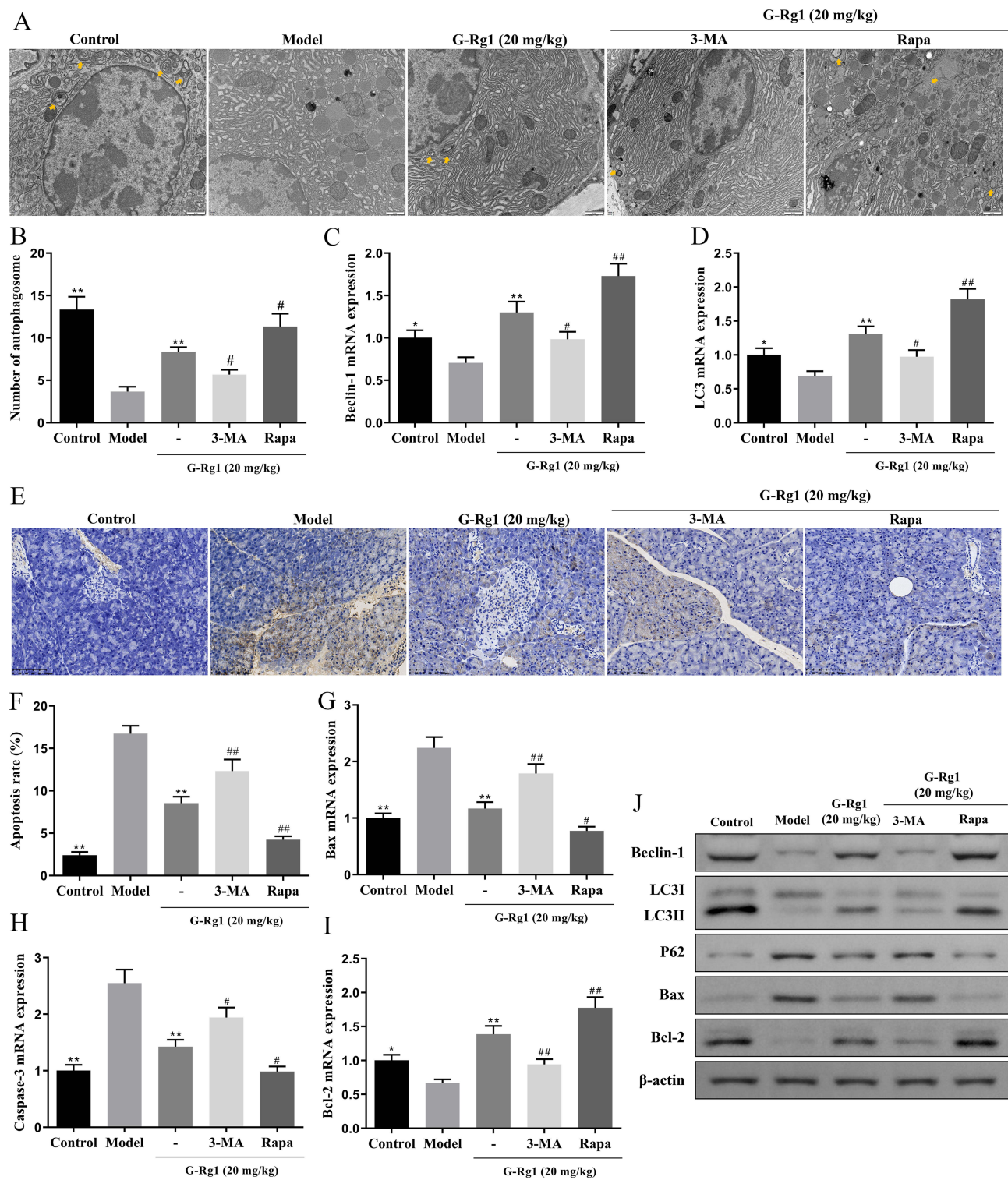


Figure 4 Effect of G-Rg1 on cell autophagy and apoptosis of pancreas in STZ-induced diabetic mice. **(A)** Representative transmission electron microscopy (TEM) images of pancreatic tissues in STZ-induced diabetic mice and **(B)** TEM quantification of autophagosomes (yellow arrows, scale bar: 1 μ m) ($n = 3$). **(C and D)** Relative expressions of Beclin-1 and LC 3 in pancreatic tissues were measured by qRT-PCR. **(E and F)** The apoptosis levels were detected by TUNEL staining (scale bar=100 μ m). **(G-I)** The levels of Bax, Caspase-3 and Bcl-2 in pancreatic tissues were determined by qRT-PCR. **(J)** Western blotting was conducted to measure the expression levels of Beclin-1, LC3, P62, Bax, and Bcl-2 in pancreatic tissues of STZ-induced diabetic mice. * $P < 0.05$, ** $P < 0.01$, compared with the model group; # $P < 0.05$, ## $P < 0.01$, compared with the G-Rg1 (20 mg/kg) group.

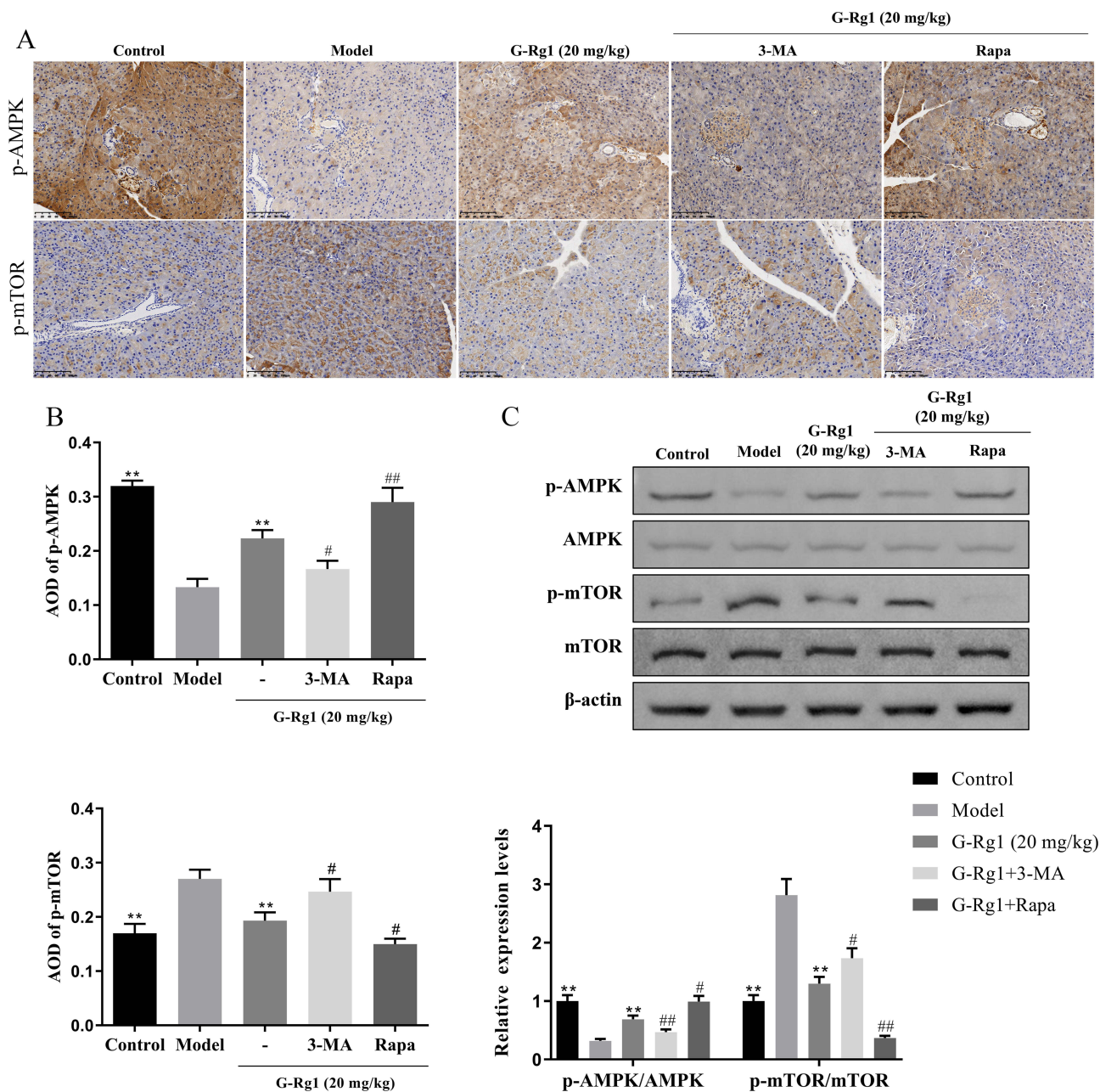


Figure 5 Effect of G-Rg1 on AMPK/mTOR pathway of the pancreas in STZ-induced diabetic mice. (A) Immunohistochemical and (B) quantitative analysis of p-AMPK and p-mTOR expressions in the pancreas of STZ-induced diabetic mice (scale bar=100 μ m). (C) The protein levels of p-AMPK, AMPK, p-mTOR, and mTOR from each group in the pancreas were measured by Western blot. ** $P<0.01$, compared with the model group; # $P<0.05$, ### $P<0.01$, compared with the G-Rg1 (20 mg/kg) group.

LC3 I, and Bcl-2, as well as raised the protein expression of p62, Bax, and Caspase-3 in HG+G-Rg1+3-MA group compared with that in the HG+G-Rg1 group (Figure 7B, $P<0.01$). According to these findings, HG-induced apoptosis in RIN-m5F cells was reduced by G-Rg1 through inducing autophagy.

G-Rg1 Attenuated Apoptosis in HG-Induced RIN-m5F Cells via Activating the AMPK

To further demonstrate the effect of G-Rg1 on apoptosis in vitro, we also investigated the therapeutic effect of G-Rg1 in HG-induced RIN-m5F cells with G-Rg1 combined with the AMPK inhibitor Compound C (CC). Flow cytometry results illustrated that the cell apoptosis levels of HG-induced RIN-m5F cells were significantly decreased in the HG+G-Rg1 treatment group. However, the CC prevented the effects of G-Rg1 on HG-induced RIN-m5F cells (Figure 8A, $P<0.01$).

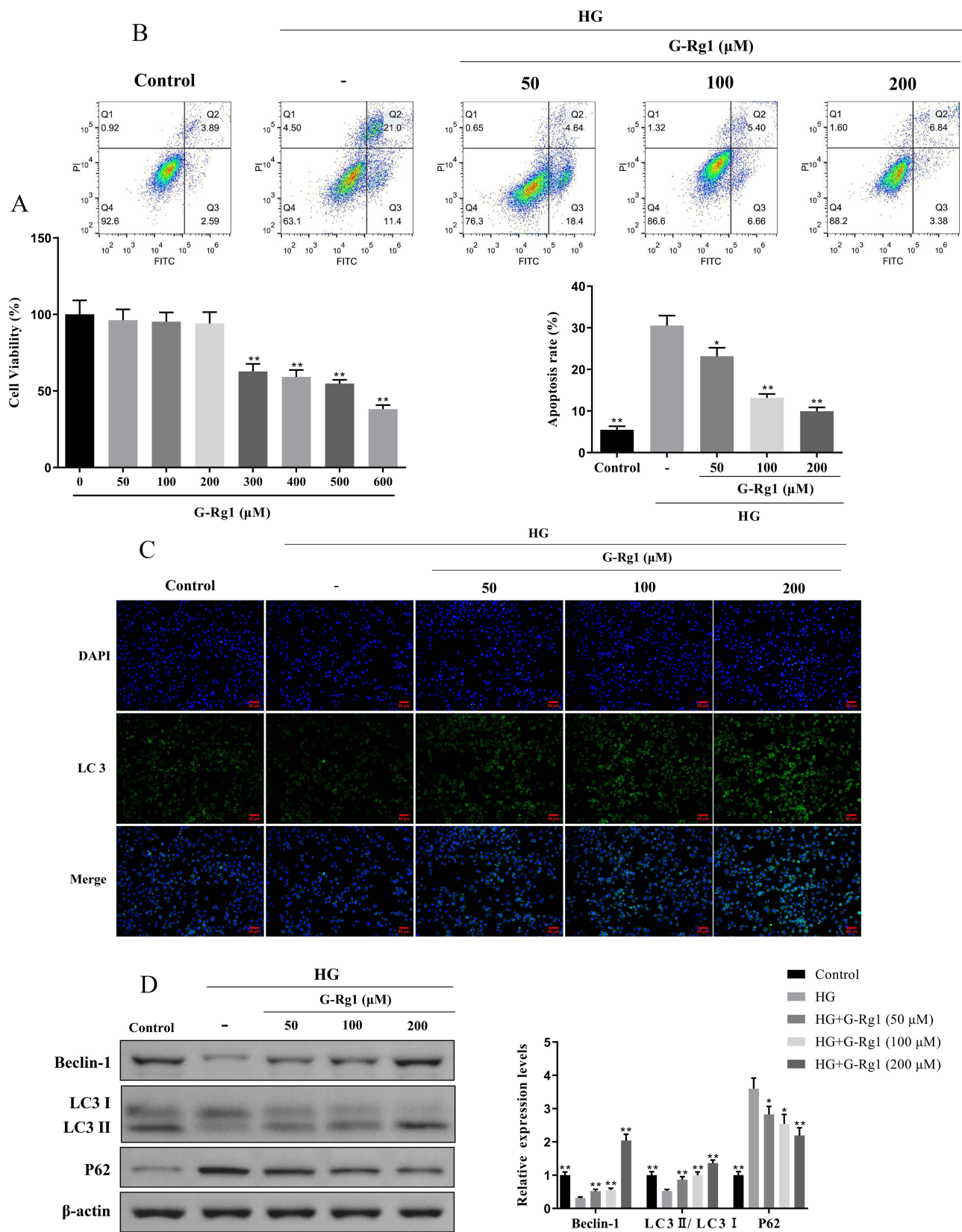


Figure 6 Effect of G-Rg1 on cell autophagy and apoptosis in high glucose (HG)-induced RIN-m5F cells. **(A)** Cell viability of RIN-m5F cells with different concentrations of G-Rg1 treatment for 24 h was measured with CCK-8 assay. **(B)** RIN-m5F cells were pre-treated with or without (50, 100, 200 μM) G-Rg1 for 24 h and then incubated with 30 mM glucose for 48 h. Then, flow cytometry was performed to assess the apoptosis rate of the HG-induced RIN-m5F cells. **(C)** The protein levels of LC 3 were detected by immunofluorescence assay (scale bar=50 μm). **(D)** Western blot was performed to assess Beclin-1, LC3, and P62 expression in HG-induced RIN-m5F cells. * $P < 0.05$, ** $P < 0.01$, compared with the HG group.

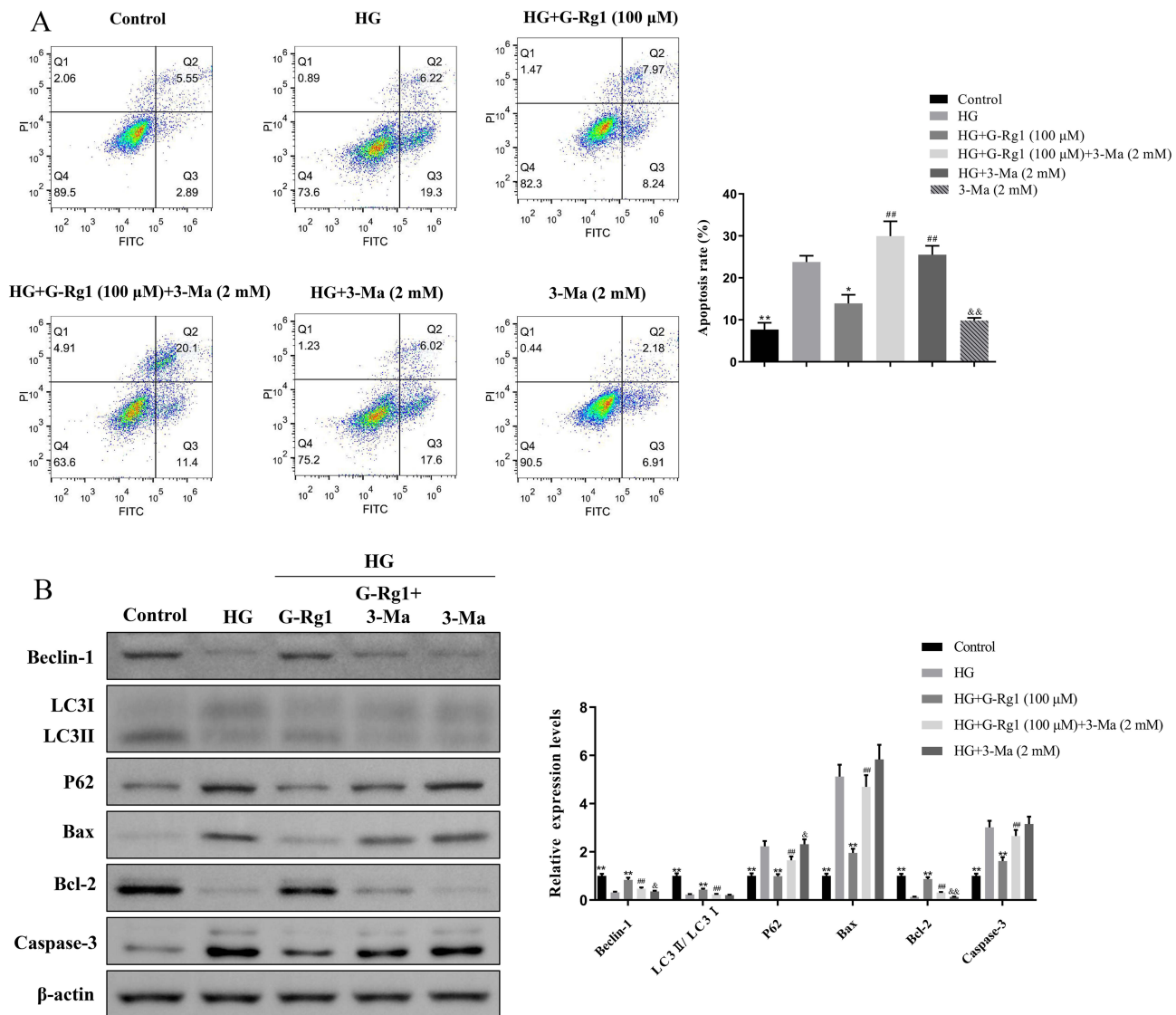


Figure 7 Effect of G-Rg1 combined with 3-MA on cell apoptosis in HG-induced RIN-m5F cells. **(A)** RIN-m5F cells were treated with 100 μ M of G-Rg1 with or without 3-MA for 24h and followed by incubated with HG for 48h. Then, cell apoptotic rates were analyzed by flow cytometry. **(B)** The expression of the autophagy and apoptosis-associated proteins, Beclin-1, LC3, P62, Bax, Bcl-2, and Caspase-3 was detected by Western blotting. * $P < 0.05$, ** $P < 0.01$, compared with the HG group. ### $P < 0.01$, compared with the HG+G-Rg1 (100 μ M) group. &P < 0.05 , &&P < 0.01 , compared with the HG+G-Rg1 (100 μ M)+3-MA (2 mM) group.

Also, CC increased the apoptosis rate in HG-induced RIN-m5F cells compared with G-Rg1 alone. Mechanically, we discovered that G-Rg1 increased p-AMPK and decreased p-mTOR levels in both low- and high-glucose situations (Figure 8B and C). Specifically, concerning Beclin-1, LC3, and p-AMPK, the inclusion of G-Rg1 weakened the CC-induced decrease of these molecules but a contrary effect of p62 was observed in the HG-induced RIN-m5F cells (Figure 8D and E). These findings demonstrated that G-Rg1 activated autophagy through the AMPK pathway, thus suppressing cell apoptosis in HG-induced RIN-m5F cells.

Discussion

Long-term increased blood glucose levels brought on by an absolute or relative insulin insufficiency are the hallmark of diabetes mellitus (DM), a metabolic disorder. According to polls, there are more than 400 million diabetes patients globally, and China has overtaken the United States as the nation with the highest total healthcare expenditures due to the disease.³⁴ Decompensation of pancreatic function occurs gradually as diabetes develops, and a high-glucose environment promotes abnormal levels of autophagy, which results in a decline of β -cell mass due to increased islet cell apoptosis.³⁵

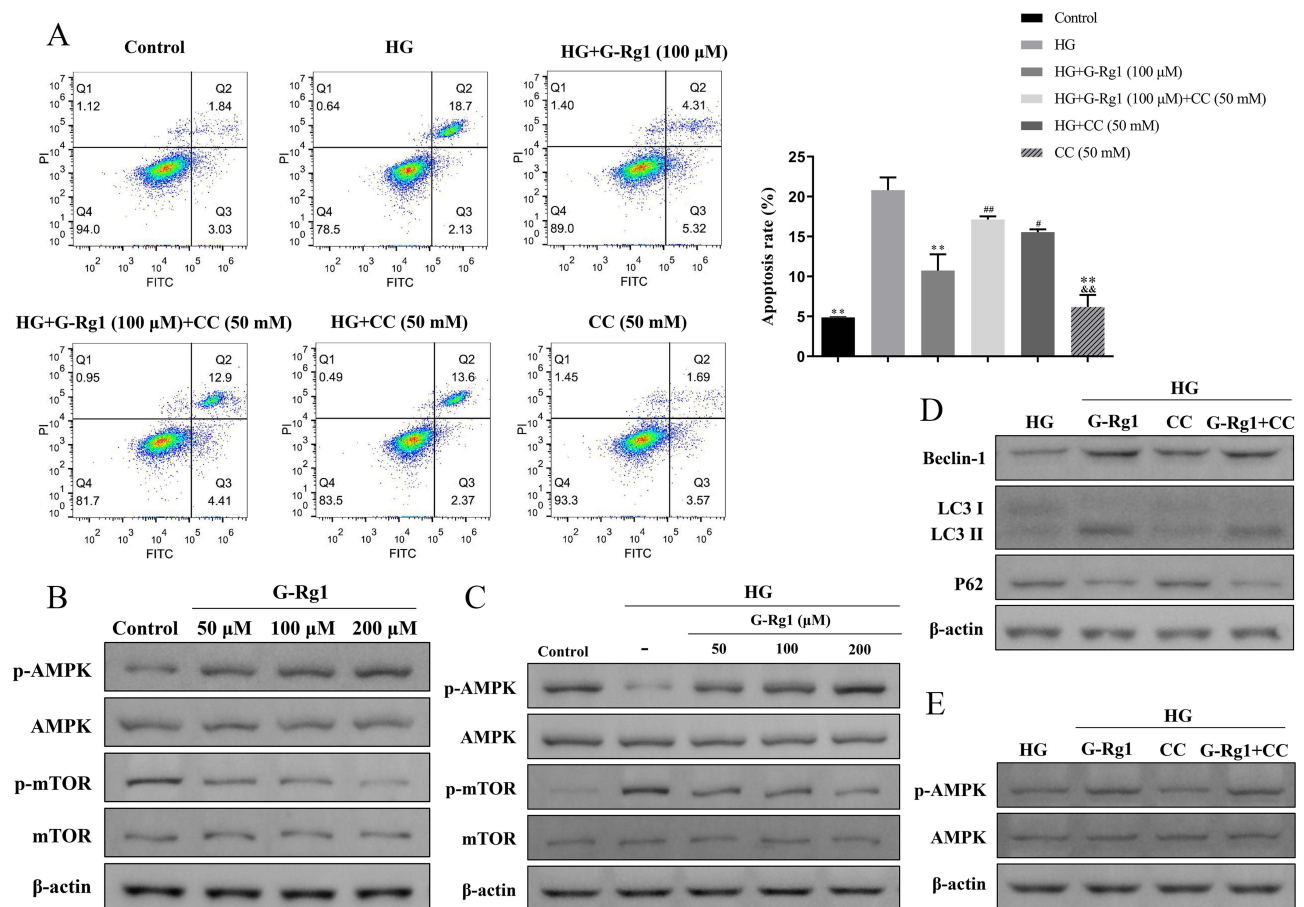


Figure 8 Effect of G-Rg1 combined with AMPK inhibitor on cell apoptosis in HG-induced RIN-m5F cells. **(A)** RIN-m5F cells were treated with 100 μM of G-Rg1 with or without AMPK inhibitor (Compound C, CC, 50 nM) for 24h and followed by incubation with HG for 48h. The apoptosis rate of HG-induced RIN-m5F cells was evaluated by flow cytometry. **(B)** The expression levels of p-AMPK, AMPK, p-mTOR and mTOR of RIN-m5F cells with conventional culture conditions were assessed by Western blotting. **(C)** The expression levels of p-AMPK, AMPK, p-mTOR and mTOR of HG-induced RIN-m5F cells under G-Rg1 treatment were assessed by Western blotting. **(D and E)** The expression levels of Beclin-1, LC3, P62, p-AMPK, and AMPK were measured with Western blot analysis in the G-Rg1 combined with CC-treated RIN-m5F cells. * $P < 0.05$, ** $P < 0.01$, compared with the HG group. # $P < 0.05$, ## $P < 0.01$, compared with the HG+G-Rg1 (100 μM) group. && $P < 0.01$, compared with the HG+CC (50 mM) group.

Hence, inhibiting pancreatic cell apoptosis and preserving pancreatic-cell function is of utmost importance in the management of diabetes. An effective component of the Chinese herbal remedies ginseng and sanqi, ginsenoside Rg1 (G-Rg1), has been utilized extensively for several diabetes problems. Previous studies suggested that G-Rg1 inhibited inflammation and oxidative stress,²³ improved intestinal microbial composition,³⁶ and alleviated fibrosis and epithelial-mesenchymal transition³⁷ in animal models and cells. However, the role of G-Rg1 on the function and survival of pancreatic β -cell needs to be further explored. In the current study, our results showed that G-Rg1 alleviated glucose and lipid metabolism levels, pancreatic islet fibrosis, and HG-induced apoptosis by promoting autophagic activity in pancreatic tissues of STZ-induced type-1 diabetes mellitus (T1DM) mice and HG-induced RIN-m5F cells. Moreover, we further found that the AMPK/mTOR pathway has a pivotal role in G-Rg1-induced autophagy in vivo and in vitro. Therefore, we have preliminarily reported that the AMPK signaling pathway, which is activated by G-Rg1, protects pancreatic cells against high-glucose conditions.

Autophagy is a highly conserved catabolic process that allows cells to recycle their extra or damaged contents, supporting cellular homeostasis and enabling cellular survival under stressful environments.³⁵ Numerous studies have examined the impact of G-Rg1 on autophagy under different conditions. For example, Zhao et al found that G-Rg1 could promote autophagy via inhibiting NF- κ B/NLRP3 inflammasome signaling pathway to improve acute liver injury in mice.³⁸ Another study found that G-Rg1 dramatically reduced renal fibrosis and podocyte epithelial-mesenchymal transition in diabetic rats by promoting the AKT/GSK3/ β -catenin pathway-mediated autophagy.³⁷ On the other side,

the inhibition of apoptosis and enhancement of autophagy in an ATG12-dependent manner were also observed in paraquat-induced epithelial cell senescence after G-Rg1 treatment.³⁹ Most importantly, islet beta cells macroautophagy/crinophagy impairment has been confirmed in human type 1 diabetes.⁴⁰ Collectively, these investigations demonstrate that autophagy is essential for a variety of physiological and pathological processes, including pancreatic β -cell function and survival.

An orderly, genetically controlled kind of cell death known as apoptosis may be the primary cause of relative insulin insufficiency in people with DM. Apoptosis occurs when pancreatic beta-cells are destroyed. As diabetes progresses, pancreatic dysfunction and islet cell loss happen in both T1DM and T2DM. The final stage in the development of T1DM, islet cell apoptosis, causes a massive decrease in islet cells and further triggers the onset of hyperglycemia.⁴¹ Islet cell apoptosis, which is the cause of both the decline in islet cell number and the rise in functional impairment, is what causes the steady increase in functional impairment and decrease in islet cell number in hyperglycemia. Therefore, inhibiting islet cell apoptosis thus becomes essential for protecting islet cells and preventing pancreatic damage in T1DM. The key regulators of apoptosis are the apoptosis-inducing gene Bax and the apoptosis-inhibiting gene Bcl-2. When the expression of these two genes is dysregulated, it activates the Caspase signaling pathway, which causes apoptosis and impairs cell function. As a result, boosting the expression of the apoptosis-inhibiting Bcl-2 protein and suppressing the expression of the apoptosis-inducing Bax protein and Caspase family protein may be key strategies for both avoiding and treating pancreatic injury in DM.

Both apoptosis and autophagic cell death are forms of planned cell death, and they share many of the regulating proteins. Both physiologic and pathologic diseases, including T1DM, may experience these processes.⁴² In this study, our results also found that the G-Rg1 and/or G-Rg1+Rapa treatment increased the number of autophagosomes and suppressed apoptosis levels in the T1DM mice model and HG-induced RIN-m5F cells, as accompanied by an up-regulation of Beclin-1, LC3, Bcl-2, as well as an inhibition of P62, Bax, and Caspase-3 expressions. Moreover, inhibition of autophagy via 3-MA can impair the anti-apoptosis effect of Rg1, demonstrating that G-Rg1 triggered autophagy, which prevented HG from inducing apoptosis in RIN-m5F cells.

The AMPK is a key regulator of biological energy metabolism and a classical upstream regulator of autophagy.⁴³ Activation of AMPK leads to the upregulation of autophagy, and AMPK is essential for cell survival and function.⁴⁴ Several studies have shown that activation of AMPK contributed to negatively regulating mTOR.^{44–46} Promoting autophagy by regulating the AMPK/mTOR signaling pathway improves myocardial fibrosis, bone regeneration, and liver injury in diabetic rats.^{47–49} In this study, the increased protein expression levels of p-AMPK/AMPK and decreased p-mTOR/mTOR levels were observed in G-Rg1-treated normal control and HG-induced RIN-m5F cells. To further investigate the direct role of G-Rg1 on the activation of AMPK in autophagy, Compound C was used in this study's cellular tests. The findings demonstrated that AMPK was activated by G-Rg1 pretreatment in comparison to the HG group, and that treatment with Compound C prevented AMPK activation, lowered the expression of Beclin1 and LC3, as well as increased the expression of p62, and also reversed the inhibitory effect of G-Rg1 on apoptosis in HG-induced RIN-m5F cells, suggesting that G-Rg1 may improve apoptosis in RIN-m5F cells by inducing autophagy via activating AMPK.

Conclusion

In summary, our work revealed that G-Rg1 may prevent T1DM by increasing autophagic activity through a potential mechanism that may be related to the AMPK/mTOR signaling pathway. This might offer a fresh theoretical foundation and experimental backing for the use of G-Rg1 in the treatment of T1DM. There are, however, some restrictions as well. First, the further mechanisms of G-Rg1 on mTOR in T1DM remain unclear. Also, there are insufficient clinical data to support the mechanistic hypothesis. Consequently, *in vivo* and *in vitro* validations of G-Rg1 on T1DM are needed for further analysis.

Data Sharing Statement

The data and materials generated or analyzed during this study are available from the corresponding author upon reasonable request.

Ethical Compliance

Research experiments conducted in this article with animals were approved by Experimental Animal Ethics Committee of Hangzhou Eyoung Biomedical Research and Development Center (No.20210214685) following all guidelines, regulations, legal, and ethical standards as required for humans or animals.

Acknowledgments

The present work was supported by the key science & technology project of medicine and health, Zhejiang province, Foundation of scientific research of national health care commission (WKJ-ZJ-2009), Science and Technology Program of Jinhua Science and Technology Bureau (2020-3-009; 2022-4-314), and Foundation of Zhejiang Provincial Education Department (Y202249904).

Disclosure

The authors declare no conflicts of interest.

References

1. Cloete L. Diabetes mellitus: an overview of the types, symptoms, complications and management. *Nurs Stand*. 2022;37(1):61–66. doi:10.7748/ns.2021.e11709
2. Syed FZ. Type 1 Diabetes Mellitus. *Ann Intern Med*. 2022;175(3):ITC33–ITC48. doi:10.7326/AITC202203150
3. Patterson CC, Karuranga S, Salpea P, et al. Worldwide estimates of incidence, prevalence and mortality of type 1 diabetes in children and adolescents: results from the international diabetes federation diabetes atlas. *Diabetes Res Clin Pract*. 2019;157:107842. doi:10.1016/j.diabres.2019.107842
4. Zhao X, Hilton A, Watson R, et al. Development and validity testing of a type 1 diabetes resource for 10–19-years old adolescents in China. *J Pediatr Nurs*. 2021;60:e96–e103. doi:10.1016/j.pedn.2021.03.029
5. Chellappan DK, Sivam NS, Teoh KX, et al. Gene therapy and type 1 diabetes mellitus. *Biomed Pharmacother*. 2018;108:1188–1200. doi:10.1016/j.biopha.2018.09.138
6. Chen S, Du K, Zou C. Current progress in stem cell therapy for type 1 diabetes mellitus. *Stem Cell Res Ther*. 2020;11(1):275. doi:10.1186/s13287-020-01793-6
7. Chen X, Affinati AH, Lee Y, et al. Immune checkpoint inhibitors and risk of type 1 diabetes. *Diabetes Care*. 2022;45(5):1170–1176. doi:10.2337/dc21-2213
8. Stamati A, Karagiannis T, Tsapas A, et al. Efficacy and safety of ultra-rapid insulin analogues in insulin pumps in patients with type 1 diabetes mellitus: a systematic review and meta-analysis. *Diabetes Res Clin Pract*. 2022;193:110144. doi:10.1016/j.diabres.2022.110144
9. Kumar K, Baliga G, Babu N, et al. Clinical features and surgical outcomes of complications of proliferative diabetic retinopathy in young adults with type 1 diabetes mellitus versus type 2 diabetes mellitus - A comparative observational study. *Indian J Ophthalmol*. 2021;69(11):3289–3295. doi:10.4103/ijo.IJO_1293_21
10. Chalakovova T, Yotov Y, Tzotchev K, et al. Type 1 diabetes mellitus - risk factor for cardiovascular disease morbidity and mortality. *Curr Diabetes Rev*. 2021;17(1):37–54. doi:10.2174/18756417MTA2pNTAa1
11. Yang B, Gan MS, Lin ZY, et al. Identification of autophagy-related genes as potential biomarkers for type 1 diabetes mellitus. *Ann Transl Med*. 2022;10(11):637. doi:10.21037/atm-22-1812
12. Bokhary K, Aljaser F, Abudawood M, et al. Role of oxidative stress and severity of diabetic retinopathy in type 1 and type 2 diabetes. *Ophthalmic Res*. 2021;64(4):613–621. doi:10.1159/000514722
13. Zhang J, Xiao Y, Hu J, et al. Lipid metabolism in type 1 diabetes mellitus: pathogenetic and therapeutic implications. *Front Immunol*. 2022;13:999108. doi:10.3389/fimmu.2022.999108
14. Muralidharan C, Linnemann AK. β -Cell autophagy in the pathogenesis of type 1 diabetes. *Am J Physiol Endocrinol Metab*. 2021;321(3):E410–E416. doi:10.1152/ajpendo.00151.2021
15. Oh SJ, Lee MS. Role of autophagy in the pathogenesis of diabetes and therapeutic potential of autophagy modulators in the treatment of diabetes and metabolic syndrome. *J Korean Med Sci*. 2022;37(37):e276. doi:10.3346/jkms.2022.37.e276
16. Šrámek J, Němcová-Fürstová V, Kovář J. Molecular mechanisms of apoptosis induction and its regulation by fatty acids in pancreatic β -cells. *Int J Mol Sci*. 2021;22(8):4285. doi:10.3390/ijms22084285
17. Saikia R, Joseph J. AMPK: a key regulator of energy stress and calcium-induced autophagy. *J Mol Med*. 2021;99(11):1539–1551. doi:10.1007/s00109-021-02125-8
18. Ji S, Zhu C, Gao S, et al. Morus alba leaves ethanol extract protects pancreatic islet cells against dysfunction and death by inducing autophagy in type 2 diabetes. *Phytomedicine*. 2021;83:153478. doi:10.1016/j.phymed.2021.153478
19. Zhou B, Leng Y, Lei SQ, et al. AMPK activation restores ischemic post-conditioning cardioprotection in STZ-induced type 1 diabetic rats: role of autophagy. *Mol Med Rep*. 2017;16(3):3648–3656. doi:10.3892/mmr.2017.7033
20. Yang F, Qin Y, Wang Y, et al. Metformin Inhibits the NLRP3 Inflammasome via AMPK/mTOR-dependent Effects in Diabetic Cardiomyopathy. *Int J Biol Sci*. 2019;15(5):1010–1019. doi:10.7150/ijbs.29680
21. Varshney R, Varshney R, Mishra R, et al. Kaempferol alleviates palmitic acid-induced lipid stores, endoplasmic reticulum stress and pancreatic β -cell dysfunction through AMPK/mTOR-mediated lipophagy. *J Nutr Biochem*. 2018;57:212–227. doi:10.1016/j.jnutbio.2018.02.017
22. Wang XY, Zhu BR, Jia Q, et al. Cinnamtannin D1 protects pancreatic β -cells from glucolipotoxicity-induced apoptosis by enhancement of autophagy in vitro and in vivo. *J Agric Food Chem*. 2020;68(45):12617–12630. doi:10.1021/acs.jafc.0c04898

23. Liu H, Chen W, Lu P, et al. Ginsenoside Rg1 attenuates the inflammation and oxidative stress induced by diabetic nephropathy through regulating the PI3K/AKT/FOXO3 pathway. *Ann Transl Med.* 2021;9(24):1789. doi:10.21037/atm-21-6234
24. Yang Y, Wang L, Zhang C, et al. Ginsenoside Rg1 improves Alzheimer's disease by regulating oxidative stress, apoptosis, and neuroinflammation through Wnt/GSK-3 β / β -catenin signaling pathway. *Chem Biol Drug Des.* 2022;99(6):884–896. doi:10.1111/cbdd.14041
25. Gao Y, Li J, Chu S, et al. Ginsenoside Rg1 protects mice against streptozotocin-induced type 1 diabetic by modulating the NLRP3 and Keap1/Nrf2/HO-1 pathways. *Eur J Pharmacol.* 2020;866:172801. doi:10.1016/j.ejphar.2019.172801
26. Yang P, Ling L, Sun W, et al. Ginsenoside Rg1 inhibits apoptosis by increasing autophagy via the AMPK/mTOR signaling in serum deprivation macrophages. *Acta Biochim Biophys Sin (Shanghai).* 2018;50(2):144–155. doi:10.1093/abbs/gmx136
27. Samarghandian S, Azimi-Nezhad M, Samini F, et al. Chrysin treatment improves diabetes and its complications in liver, brain, and pancreas in streptozotocin-induced diabetic rats. *Can J Physiol Pharmacol.* 2016;94(4):388–393. doi:10.1139/cjpp-2014-0412
28. Lan ZJ, Lei Z, Nation L, et al. Oral administration of NPC43 counters hyperglycemia and activates insulin receptor in streptozotocin-induced type 1 diabetic mice. *BMJ Open Diabetes Res Care.* 2020;8(1):e001695. doi:10.1136/bmjdr-2020-001695
29. Liu H, Wang J, Liu M, et al. Antiobesity Effects of Ginsenoside Rg1 on 3T3-L1 Preadipocytes and high fat diet-induced obese mice mediated by AMPK. *Nutrients.* 2018;10(7):830. doi:10.3390/nu10070830
30. Xiao Y, Wu QQ, Duan MX, et al. TAX1BP1 overexpression attenuates cardiac dysfunction and remodeling in STZ-induced diabetic cardiomyopathy in mice by regulating autophagy. *Biochim Biophys Acta Mol Basis Dis.* 2018;1864(5 Pt A):1728–1743. doi:10.1016/j.bbdis.2018.02.012
31. Baeyens A, Pérol L, Fourcade G, et al. Limitations of IL-2 and rapamycin in immunotherapy of type 1 diabetes. *Diabetes.* 2013;62(9):3120–3131. doi:10.2337/db13-0214
32. Wang W, Xu AL, Li ZC, et al. Combination of probiotics and salvia miltiorrhiza polysaccharide alleviates hepatic steatosis via gut microbiota modulation and insulin resistance improvement in high fat-induced NAFLD mice. *Diabetes Metab J.* 2020;44(2):336–348. doi:10.4093/dmj.2019.0042
33. Rao X, Huang X, Zhou Z, et al. An improvement of the 2 $\Delta\Delta$ CT method for quantitative real-time polymerase chain reaction data analysis. *Biostat Bioinforma Biomath.* 2013;3(3):71–85.
34. Saeedi P, Petersohn I, Salpea P, et al. Global and regional diabetes prevalence estimates for 2019 and projections for 2030 and 2045: results from the international diabetes federation diabetes atlas. *Diabetes Res Clin Pract.* 2019;157:107843. doi:10.1016/j.diabres.2019.107843
35. Marasco MR, Linnemann AK. β -Cell Autophagy in Diabetes Pathogenesis. *Endocrinology.* 2018;159(5):2127–2141. doi:10.1210/en.2017-03273
36. Peng M, Wang L, Su H, et al. Ginsenoside Rg1 improved diabetes through regulating the intestinal microbiota in high-fat diet and streptozotocin-induced type 2 diabetes rats. *J Food Biochem.* 2022;46(10):e14321. doi:10.1111/jfbc.14321
37. Shi Y, Gao Y, Wang T, et al. Ginsenoside Rg1 Alleviates Podocyte EMT Passage by Regulating AKT/GSK3 β / β -Catenin Pathway by Restoring Autophagic Activity. *Evid Based Complement Alternat Med.* 2020;2020:1903627. doi:10.1155/2020/1903627
38. Zhao J, He B, Zhang S, et al. Ginsenoside Rg1 alleviates acute liver injury through the induction of autophagy and suppressing NF- κ B/NLRP3 inflammasome signaling pathway. *Int J Med Sci.* 2021;18(6):1382–1389. doi:10.7150/ijms.50919
39. Huang C, Xue X, Gong N, et al. Ginsenoside Rg1 suppresses paraquat-induced epithelial cell senescence by enhancing autophagy in an ATG12-dependent manner. *Environ Toxicol.* 2022;37(9):2302–2313. doi:10.1002/tox.23597
40. Muralidharan C, Conteh AM, Marasco MR, et al. Pancreatic beta cell autophagy is impaired in type 1 diabetes. *Diabetologia.* 2021;64(4):865–877. doi:10.1007/s00125-021-05387-6
41. Chwalba A, Piłśniak A, Otto-Buczowska E. β -cell self-destruction and extremely complicated and still unknown etiopathogenesis of type 1 diabetes. Proces autodestrukcji komórek β trzustki oraz niezwykle skomplikowana i wciąż nieznana etiopatogeneza cukrzycy typu 1. *Pediatr Endocrinol Diabetes Metab.* 2021;27(1):47–50. doi:10.5114/pedm.2020.103058
42. Demirtas L, Guclu A, Erdur FM, et al. Apoptosis, autophagy & endoplasmic reticulum stress in diabetes mellitus. *Indian J Med Res.* 2016;144(4):515–524. doi:10.4103/0971-5916.200887
43. Li Y, Chen Y. AMPK and Autophagy. *Adv Exp Med Biol.* 2019;1206:85–108.
44. Moore MN. Lysosomes, Autophagy, and Hormesis in Cell Physiology, Pathology, and Age-Related Disease. *Dose Response.* 2020;18(3):1559325820934227. doi:10.1177/1559325820934227
45. Wang Y, Liu Z, Shu S, et al. AMPK/mTOR signaling in autophagy regulation during cisplatin-induced acute kidney injury. *Front Physiol.* 2020;11:619730. doi:10.3389/fphys.2020.619730
46. Li Y, Sun R, Zou J, et al. Dual roles of the AMP-activated protein kinase pathway in angiogenesis. *Cells.* 2019;8(7):752. doi:10.3390/cells8070752
47. Chen M, Jing D, Ye R, et al. PPAR β / δ accelerates bone regeneration in diabetic mellitus by enhancing AMPK/mTOR pathway-mediated autophagy. *Stem Cell Res Ther.* 2021;12(1):566. doi:10.1186/s13287-021-02628-8
48. Zhang Y, Ling Y, Yang L, et al. Liraglutide relieves myocardial damage by promoting autophagy via AMPK-mTOR signaling pathway in Zucker diabetic fatty rat. *Mol Cell Endocrinol.* 2017;448:98–107. doi:10.1016/j.mce.2017.03.029
49. Zhu Y, Su Y, Zhang J, et al. Astragaloside IV alleviates liver injury in type 2 diabetes due to promotion of AMPK/mTOR-mediated autophagy. *Mol Med Rep.* 2021;23(6):437. doi:10.3892/mmr.2021.12076

Diabetes, Metabolic Syndrome and Obesity

Dovepress

Publish your work in this journal

Diabetes, Metabolic Syndrome and Obesity is an international, peer-reviewed open-access journal committed to the rapid publication of the latest laboratory and clinical findings in the fields of diabetes, metabolic syndrome and obesity research. Original research, review, case reports, hypothesis formation, expert opinion and commentaries are all considered for publication. The manuscript management system is completely online and includes a very quick and fair peer-review system, which is all easy to use. Visit <http://www.dovepress.com/testimonials.php> to read real quotes from published authors.

Submit your manuscript here: <https://www.dovepress.com/diabetes-metabolic-syndrome-and-obesity-journal>